Current Optics and Photonics
Vol. 3, No. 6, December 2019, pp. 583-589

ISSN: 2508-7266(Print) / ISSN: 2508-7274(Online)
DOI: https://doi.org/10.3807/COPP.2019.3.6.583

# 940-nm 350-mW Transverse Single-mode Laser Diode with AlGaAs/InGaAs GRIN-SCH and Asymmetric Structure

**Jeonggeun Kwak*, Jongkeun Park, Jeonghyun Park, Kijong Baek, Ansik Choi, and Taekyung Kim**

*Quantum Semiconductor International (QSI), Cheonan 31044, Korea*

(Received August 8, 2019 : revised October 14, 2019 : accepted October 14, 2019)

We report experimental results on 940-nm 350-mW AlGaAs/InGaAs transverse single-mode laser diodes (LDs) adopting graded-index separate confinement heterostructures (GRIN-SCH) and *p,n*-clad asymmetric structures, with improved temperature and small-divergence beam characteristics under high-output-power operation, for a three-dimensional (3D) motion-recognition sensor. The GRIN-SCH design provides good carrier confinement and prevents current leakage by adding a grading layer between cladding and waveguide layers. The asymmetric design, which differs in refractive-index distribution of *p-n* cladding layers, reduces the divergence angle at high-power operation and widens the transverse mode distribution to decrease the power density around emission facets. At an optical power of 350 mW under continuous-wave (CW) operation, Gaussian narrow far-field patterns (FFP) are measured with the full width at half maximum vertical divergence angle to be 18 degrees. A threshold current ($I_{th}$) of 65 mA, slope efficiency (SE) of 0.98 mW/mA, and operating current ($I_{op}$) of 400 mA are obtained at room temperature. Also, we could achieve catastrophic optical damage (COD) of 850 mW and long-term reliability of 60°C with a TO-56 package.

*Keywords* : Laser diode, 940 nm laser diode, AlGaAs/InGaAs GRIN-SCH, Asymmetric structure, 3D motion recognition light source
*OCIS codes* : (250.5960) Semiconductor lasers; (280.3420) Laser sensors; (280.4788) Optical sensing and sensors

## I. INTRODUCTION

AlGaAs based semiconductor laser diodes (LDs) in the 800~900-nm band are widely used as illumination light sources for augmented reality (AR), virtual reality (VR), and 3D depth sensors, and applied to various industries such as automobile, security, and games, as shown in Fig. 1 [1, 2].

Generally a laser diode of the 800-nm band is used as an illuminating light source for indoor 3D depth sensors, but the recent popularity of facial recognition in the fields of mobile phones and security, a high-power laser diode of the 940-nm band is required for an outdoor environment. Compared to the 800-nm band, the 940-nm band has the advantage of less interference from sunlight, but the output must be increased, because the sensitivity of commercial Si detectors is low [1-4].

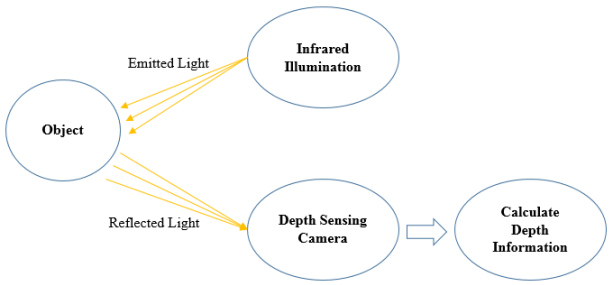


FIG. 1. Principle for 3D sensing using an infrared illumination source.

To develop a high-power LD of 940 nm, it is necessary to increase the near-field (NF) emission beam size to

*Corresponding author: jgkwak@qsilaser.com, ORCID 0000-0002-7723-7853
Color versions of one or more of the figures in this paper are available online.

reduce the heat generated by the antireflection (AR) facet; this is mainly determined by the epitaxial (EPI) design and growth technology. Normally, the narrow emission of optical power density in the NF of an LD would contribute to a low COD, and would degrade reliability. Therefore, NF beam size must be enlarged and optical density must be reduced, to improve the COD level and reliability [5]. In addition, the high-power LD must have reduced internal resistance, to suppress the heat dissipation that occurs when the output and temperature rise [6].

For high-power LDs, introducing a large optical cavity (LOC) into the separate confinement heterostructure (SCH) epitaxial layers was adopted as the simplest method to increase power and COD level. However, LOC LDs exhibit deteriorated performance, such as increase of $I_{th}$ and decrease of SE, because of the large cavity [7]. On the other hand, the double-barrier separate confinement heterostructures (DBSCH), which insert a barrier with a low refractive index between the waveguide and cladding layers, possess superior characteristics in both COD level and reliability. The DBSCH also show deterioration of LD performance, though, in slope efficiency and resistance [8, 9]. Therefore, the LOC LDs and DBSCH have limitations in obtaining output of several hundred mW, due to higher threshold and resistance values caused by the deterioration of optical confinement [5].

To solve the conventional problems, a 940-nm high-power LD has been developed as follows. First, we adopted the GRIN-SCH structures of an AlGaAs/InGaAs single quantum well (SQW) with a grading layer between cladding and waveguide layers, to improve carrier confinement and decrease optical confinement, with low far-field vertical (FFV) angle. This is one of the structures that effectively confines high power in the lasing mode, and limits the heating effects that occur at high optical intensities, such as catastrophic optical damage or spatial hole burning [10].

After that, based on the GRIN-SCH structure, an asymmetric structure was applied to broaden the optical-mode distribution to the *n*-side region, by varying the Al composition and thickness of the *p,n*-clad layers. This structure dramatically reduces the FFV and increases the COD level. Although $I_{th}$ can increase due to optical-confinement reduction, $I_{op}$ will be similar to that of the symmetric structure, due to the increase of SE [6, 11, 12]. In addition, the doing of *p,n*-clad layers is optimized to reduce series resistance and minimize free-carrier absorption.

In this study, we report graded-index separate confinement heterostructures (GRIN-SCH) that provide good carrier confinement, and an asymmetric structure that reduces FFV angle to increase COD level. These structural concepts and advantages under high-power high-reliability operation are demonstrated for 940-nm 350-mW AlGaAs/InGaAs transverse single-mode laser diodes.

## II. DESIGN

The grown epitaxial laser structure is a hetero-*p-i-n* junction. The epitaxial layer was grown by Aixtron AIX-2400 G2 metal-organic chemical vapor deposition (MOCVD) reactor at 100 mbar and 700°C. TMGa and TMAl are used as group-III sources and $AsH_3$ as the group-V hydride. Cabon and silicon are used as *p*-type and *n*-type dopants respectively. Table 1 and Fig. 2 present the layers and transmission electron microscopy (TEM) image of the 940-nm 350-mW transverse single-mode LD.

3-inch *n*-type GaAs was used as a substrate, and 1.0-μm *n*-GaAs buffer, 4.0-μm *n*-AlGaAs lower cladding layer

TABLE 1. Layers of the 940-nm 350-mW transverse single-mode laser diode

| No. | Layer | GRINSCH | | GRINSCH + Asymmetric | | Dopant |
|---|---|---|---|---|---|---|
| | | Material | Thickness (μm) | Material | Thickness (μm) | |
| 13 | *p*-contact | GaAs | 3.0000 | GaAs | 3.0000 | C |
| 12 | CBL | $Al_{0.45}GaAs$ | 0.8000 | $Al_{0.45}GaAs$ | 0.8000 | C |
| 11 | CAP | GaAs | 0.2000 | GaAs | 0.2000 | C |
| 10 | *p*-cladding | $Al_{0.35}GaAs$ | 1.3000 | $Al_{0.35}GaAs$ | 1.3000 | C |
| 9 | Etch Stop | $Al_{0.8}GaAs$ | 0.0100 | $Al_{0.8}GaAs$ | 0.0100 | C |
| 8 | H-cladding | $Al_{0.35}GaAs$ | 0.2000 | $Al_{0.35}GaAs$ | 0.2000 | C |
| 7 | *p*-waveguide | $Al_{0.15\rightarrow0.35}GaAs$ | 0.1000 | $Al_{0.15\rightarrow0.35}GaAs$ | 0.1000 | |
| 6 | Quantum Well | $In_{0.1}GaAs$ | 0.0075 | $In_{0.1}GaAs$ | 0.0075 | |
| 5 | *n*-waveguide | $Al_{0.35\rightarrow0.15}GaAs$ | 0.1000 | $Al_{0.28\rightarrow0.15}GaAs$ | 0.1000 | |
| 4 | *n*-cladding | $Al_{0.35}GaAs$ | 2.0000 | $Al_{0.28}GaAs$ | 4.0000 | Si |
| 3 | Grading | $Al_{0.35}GaAs \leftarrow GaAs$ | 0.0500 | $Al_{0.28}GaAs \leftarrow GaAs$ | 0.0500 | Si |
| 2 | Buffer | GaAs | 1.0000 | GaAs | 1.0000 | Si |
| 1 | Substrate | GaAs | - | GaAs | - | Si |

with Si as the *n*-type dopant, undoped quantum well active region, 0.2-μm *p*- AlGaAs 1st upper cladding layer, 100-Å *p*-AlGaAs etch-stop layer, 1.3-μm *p*-AlGaAs 2nd upper cladding layer with C as the *p*-type dopant, and 0.3-μm p-GaAs cap layer with C doped at a high level were successively grown in MOCVD. The undoped quantum well active region consists of 2000 Å of AlGaAs of the upper and lower waveguide layers as graded, and a 75-Å InGaAs single quantum well. The target EL wavelength was 940 nm.

The fabrication process was made with a regrowth type of selective buried ridge (SBR), growing a 0.8-μm *n*-AlGaAs current-blocking layer (CBL) and 3-μm p-GaAs 3rd growth after the ridge etch. For high-power single-mode oscillation, the stripe width was set to be 4 μm and the cavity length was chosen as 1 500 μm. For the metallization, Ti/Pt/Au was used for the *p*-side and Au-Ge/Ni/Au for the *n*-side contact respectively.

The facets were antireflection (AR) / high-reflection (HR), coated by sputter. AR reflection was 5% with $Al_2O_3/SiO_2$ layers, and HR reflection was 95% with $Al_2O_3/Si/SiO_2/Si_3N_4$ multilayers.

In this paper, we calculated and compared the mode profiles of GRIN-SCH symmetric and asymmetric vertical waveguide structures using the transfer-matrix method (TMM) [13]. Based on the TMM simulation, the 940-nm 350-mW transverse single-mode LD was implemented and evaluated.

First of all, the GRIN-SCH structures, by inserting a grading layer between the waveguide and the cladding layers based on SCH design, enhance carrier confinement while keeping the carriers in the lower grading region of the active layer [5, 10]. At the same time, the optical confinement is reduced by broadening the optical-mode distribution, due to the difference in effective refractive index in the waveguide. To obtain suitable GRIN-SCH LD performance, we adjusted the Al composition and thickness of the grading region. As a result of the TMM simulation, an FFV angle of 27° and confinement of 0.0298 were obtained, as shown in Fig. 3.

After that, to achieve the desired power level and reliability, we adopted asymmetric structures that increase the thickness and refractive index of the *n*-clad layers, to

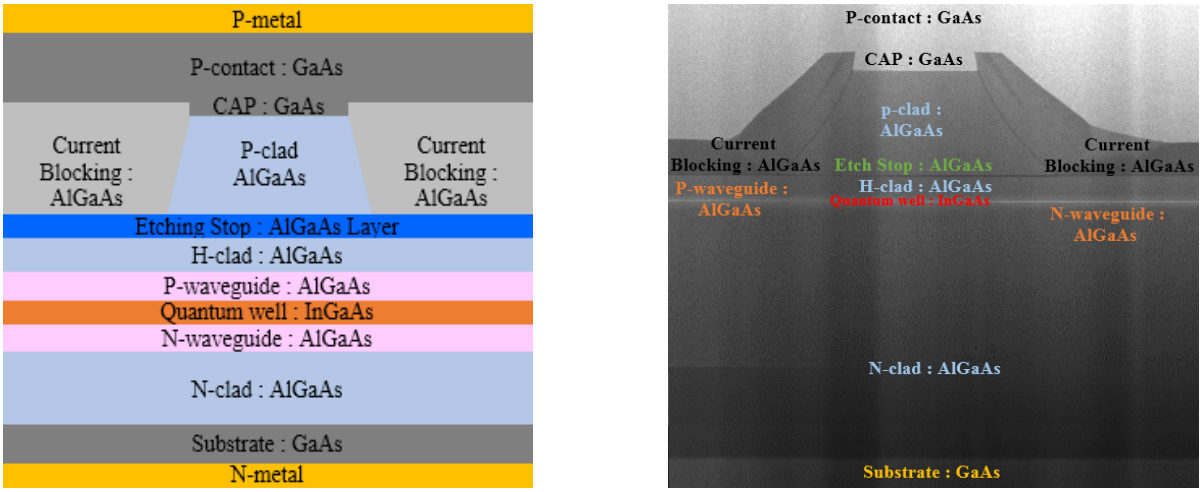


(a) (b)

FIG. 2. The 940-nm high-power laser diode of SBR type: (a) Schematic of SBR, (b) TEM image.

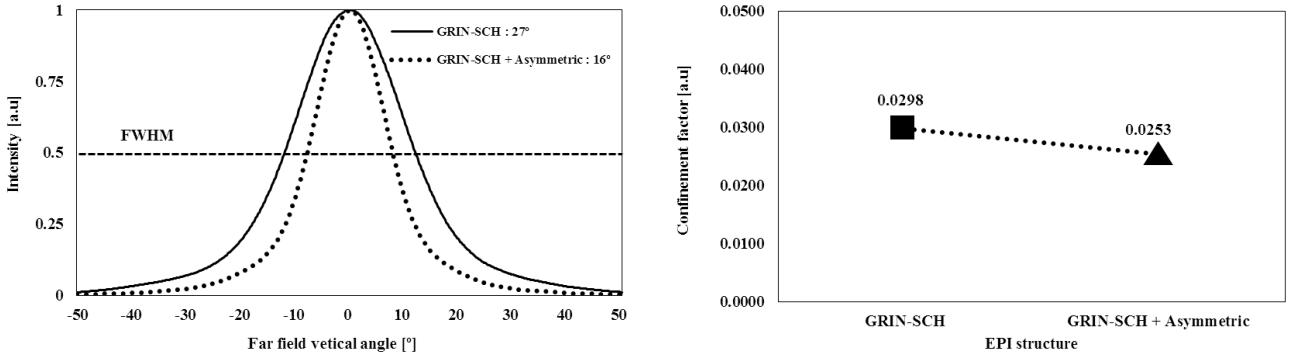


(a) (b)

FIG. 3. Simulation results for the GRIN-SCH and Asymmetric + GRIN-SCH structures: (a) FFV angle, (b) Confinement.

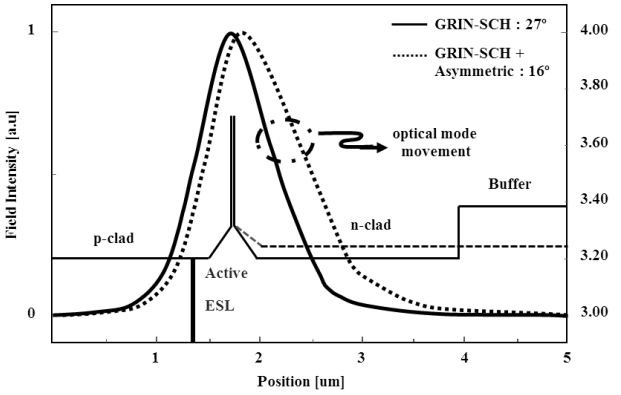


FIG. 4. Simulation results of the optical-mode distribution for asymmetric structures.

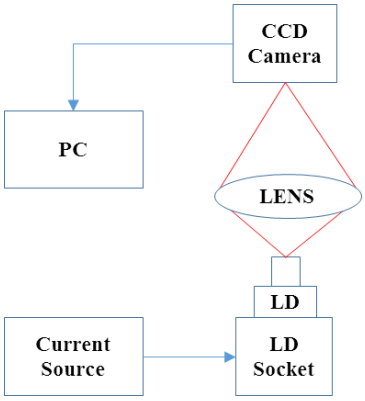


FIG. 5. Schematic diagram of the near-field measurement.

expand the optical mode more into the *n*-clad. This method can reduce the far-field divergence angle, by enlarging the optical-near-field distribution [6, 11, 12]. As a result, the asymmetric waveguide structure has a higher COD level by reducing optical intensity at the front facet, and lower internal loss because the absorption coefficient of the *p*-doped layer is lower than that of the *n*-doped layer [11]. In the TMM simulation, by changing the Al composition and thickness of the *p,n*-clad layers, the FFV can be reduced to 16° and the optical mode can be expanded into the *n*-side, as shown in Fig 4.

The doping concentration of the two structures was optimized to increase the high-power laser's efficiency and reliability, by reducing internal resistance and free-carrier absorption loss.

After the fabrication process was complete, the wafer was cleaved into chips. The AR/HR facets were coated by sputter with $Al_2O_3$, Si, $SiO_2$, and $Si_3N_4$ multilayers for high-power operation. The coated chips were assembled with TO-56 package (PKG) and evaluated for electrical-optical properties and high-temperature reliability.

## III. EXPERIMENTAL RESULTS

The 940-nm 350-mW transverse single-mode laser diode was evaluated for electrical-optical (E-O) characteristics at room temperature and reliability at high temperature in the TO-56 PKG. Output power-current-voltage (*L-I-V*), far-field horizontal (FFH), FFV, and wavelength characteristics were measured by the CW driving method using DENKEN's DKLDC330 equipment in Japan. The high-temperature (60°C) reliability was measured under auto-power-control (APC) driving conditions using BLUE'ENG's AIO9220 system in Korea. As shown in Fig. 5, near-field (NF) fundamental-mode beam profiles were imaged by a source meter (Keithley 2400) and CCD camera (WinCamD-UCD23, Datalay).

### 3.1. GRIN-SCH Structure

Figure 6 shows the evaluation results for a GRIN-SCH structure that minimizes confinement loss while reducing the FFV, by grading Al composition and thickness between waveguide and cladding layers. For output power of 350 mW, we obtained $I_{th}$ of 20 mA, $I_{op}$ of 465 mA, and FFV angle of 27°, under continuous-wave operation at room temperature.

The GRIN-SCH structure enhances carrier confinement by keeping the carriers well under the active layer, and the

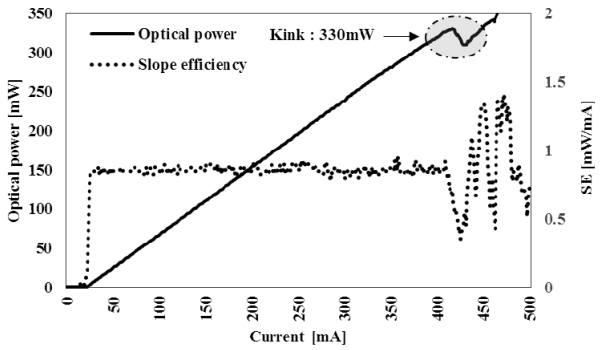


(a)

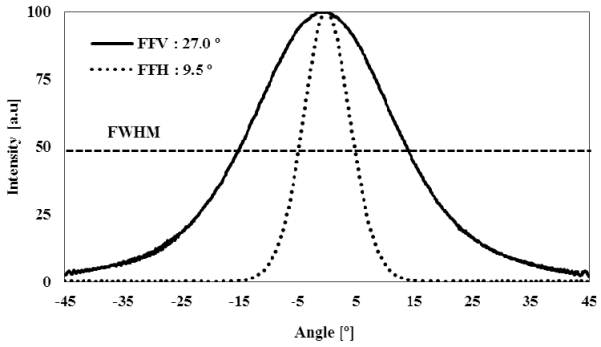


(b)

FIG. 6. *L-I* curve and FFP of the GRIN-SCH structure at 940 nm and 350 mW: (a) *L-I* measurement graph, (b) FFV measurement graph.

optical confinement of the facet surface where the beam is emitted can be reduced by decreasing the effective refractive-index difference. As a result, the output power is stable up to 330 mW and kink-free at room temperature, but there is a problem in that a kink is generated at output higher than 330 mW.

### 3.2. GRIN-SCH + Asymmetric Structure

For the GRIN-SCH structure, the characteristics of 940 nm and 330 mW class were obtained. However, there is a need to increase the power level such as kink and COD for stable illumination sources applied in outdoor optical 3D depth sensors. For this purpose, a high-power, high-reliability single-mode device must essentially reduce the FFV. Therefore an asymmetric structure based on the GRIN-SCH was adopted, by adjusting the Al composition and thickness of the *p,n*-clad layers.

As shown in Fig. 7, for an output power of 350 mW the asymmetric structure was able to obtain an FFV angle of 18°, which is about 9° less than the 27° of the GRIN-SCH structure. $I_{th}$ increased to 65 mA due to the decrease of optical confinement with the features of the asymmetric structure, the SE increased to 0.98 mW/mA, and $I_{op}$ was 400 mA, superior to the GRIN-SCH structure because of being kink-free.

Figure 8 shows the diode laser's NF fundamental mode beam profile. Intensity profiles are shown for GRIN-SCH (symmetric) and asymmetric structures with similar waveguide thicknesses. It can be seen that by asymmetric design the near-field distribution in the laser cavity is different from that of the GRIN-SCH design. In the asymmetric design, the beam intensity penetrates into the *n*-cladding layer, and the beam size was enlarged. Therefore, it can be concluded that the asymmetric structure has been successfully designed.

In addition, as the doping of the *p,n*-clad layers increased, the internal resistance decreased, and the heat dissipation characteristics were improved under high-temperature and high-power driving [12, 14].

We were able to develop a 940-nm 350-mW high-reliability laser diode. Table 2 shows the electrical and optical properties of the final laser diode. Figure 9 shows the average COD levels for the GRIN-SCH (for 10 samples) and for the asymmetric structure based on the GRIN-SCH (also for 10 samples). The asymmetric structure enhanced the slope efficiency by reducing internal loss, and by reducing the electrical and thermal resistivities of the diode laser [11]. Figure 10 shows the high-temperature reliability of the asymmetric structure based on the GRIN-SCH (for 10 samples).

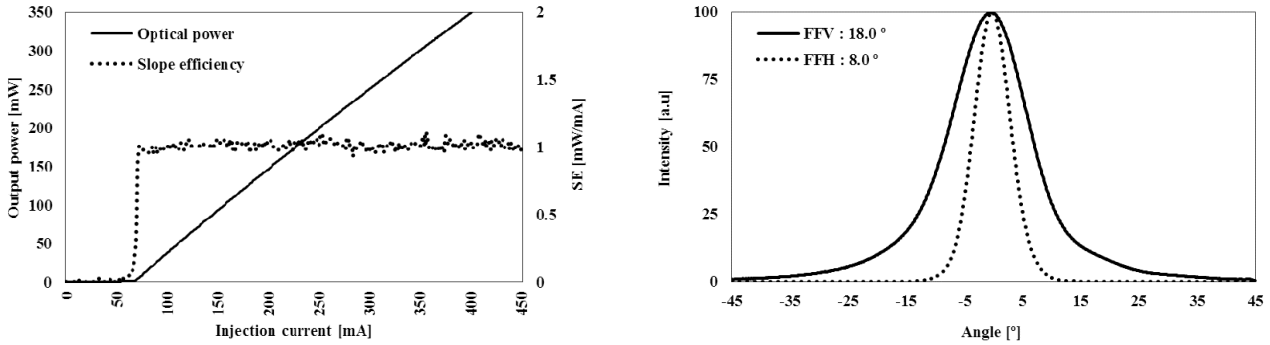


(a) (b)

FIG. 7. *L-I* curve and FFP of the asymmetric structure at 940 nm and 350 mW: (a) *L-I* measurement graph, (b) FFV measurement graph.

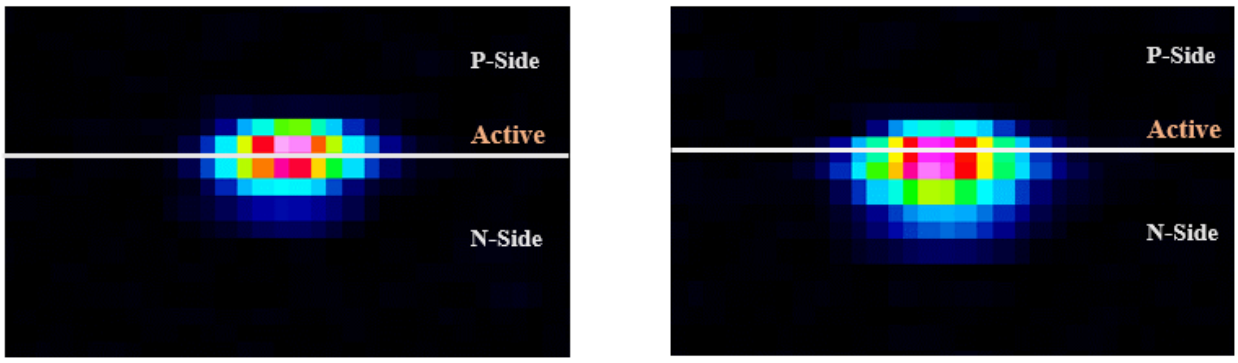


(a) (b)

FIG. 8. NF beam profiles of the GRIN-SCH and asymmetric structures: (a) GRIN-SCH, (b) GRIN-SCH + Asymmetric.

TABLE 2. E-O characteristic results for the 940-nm 350-mW laser diodes

| Structure | $V_{op}$ [V] | $I_{op}$ [mA] | $I_{th}$ [mA] | SE [W/A] | FFV [°] | FFH [°] | Wavelength [nm] |
|---|---|---|---|---|---|---|---|
| GRIN-SCH | 2.27 | 465 | 20 | - (kink) | 27.0 | 9.5 | 946 |
| GRIN-SCH + Asymmetric | 1.95 | 400 | 65 | 0.98 | 18.0 | 8.0 | 945 |

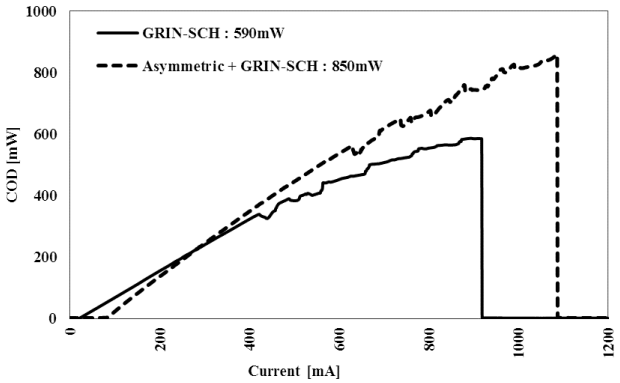


FIG. 9. Average COD levels for the GRIN-SCH and asymmetric structure based on the GRIN-SCH.

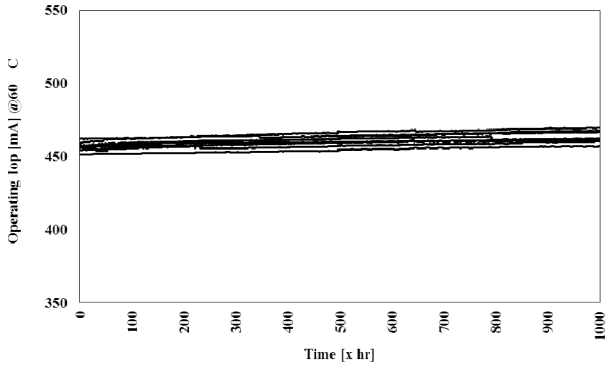


FIG. 10. 60°C reliability results for the asymmetric structure based on the GRIN-SCH.

## IV. CONCLUSION

In this paper, the results of the development of a 940-nm high-power high-reliability device, used for an outdoor 3D depth sensor, were discussed and proved. The GRIN-SCH structure has excellent carrier confinement characteristics while preventing current leakage, and the asymmetric structure based on the GRIN-SCH design has excellent COD characteristics while reducing the far-field vertical angle. By applying these two structures, the laser efficiency was maximized, because the internal loss was minimized.

We finally succeeded in developing a 940-nm 350-mW transverse single-mode LD with high reliability that can guarantee operation in a 60°C environment and a COD level of 850 mW.

## ACKNOWLEDGMENT

This work was supported by the Ministry of Trade, Industry, and Energy, Korea, under the Global Convergence Advanced Technology Center Program (Project No. 2000 1514).

## REFERENCES

1. X. Miao, D. Yum, Z. L. Brand, and H. Dahlkamp, "Method and system for using light emission by a depth-sensing camera to capture video images under low-light conditions," U.S. Patent 10,009,554 (2018).
2. R. K. Price, M. Bleyer, and D. Demandolx, "Multi-spectrum illumination-and-sensor module for head tracking, gesture recognition and spatial mapping," U.S. Patent Appl. 15/447064 (2018).
3. OSRAM Marketing IR APAC, *Wide IR Illumination & Sensing Products from OSRAM* (Consumer Applications_ Illumination & Sensing, April 2016), http://www.ledtaiwan.org/zh/sites/ledtaiwan.org/files/data16/images/%281%29IR%2BUV-S1-%20General%20Info%20Pack_Apr%272016.pdf (2018).
4. Lumentum Marketing IR, *Diode Lasers in Next-Generation 3D Sensing Applications: Meeting the Challenges of Reliability and Scale* (MARKETS_3D Sensing_ WHITE PAPER, 2018), https://resource.lumentum.com/s3fs-public/technical-library-items/diodelaser3d-wp-cl-ae.pdf (2018).
5. C. T. Hung and T. C. Lu, "830-nm AlGaAs-InGaAs graded index double barrier separate confinement heterostructures laser diodes with improved temperature and divergence characteristics," IEEE J. Quantum Electron. **49**, 127-132 (2013).
6. Y. Yamagata, Y. Yamada, M. Muto, S. Sato, R. Nogawa, A. Sakamoto, and M. Yamaguchi, "915 nm high-power broad area laser diodes with ultra-small optical confinement based on Asymmetric Decoupled Confinement Heterostructure (ADCH)," Proc. SPIE **9348**, 93480F (2015).
7. A. Knauer, G. Erbert, R. Staske, B. Sumpf, H. Wenzel, and M. Weyers, "High-power 808 nm lasers with a super-large optical cavity," Semicond. Sci. Technol. **20**, 621 (2005).
8. A. Malag and B. Mroziewicz, "Vertical beam divergence of double-barrier multiquantum well (DBMQW) (AlGa)As heterostructure lasers," J. Lightwave Technol. **14**, 1514-1518 (1996).
9. G. Lin, S.-T. Yen, C.-P. Lee, and D.-C. Liu, "Extremely small vertical far-field angle of InGaAs-AlGaAs quantum-well lasers with specially designed cladding structure," IEEE Photon. Technol. Lett. **8**, 1588-1590 (1996).
10. T. Chan, S. H. Son, K. C. Kim, and T. G. Kim, "Design

and simulation of an 808 nm InAlAs/AlGaAs GRIN-SCH quantum dot laser diode," J. Opt. Soc. Korea **15**, 124-127 (2011).
11. S. P. Abbasi and M. H. Mahdieh, "Asymmetric, non-broadened waveguide structures for double QW high-power 808 nm diode laser," Proc. SPIE **10254**, 1025406 (2017).
12. D. Heo, I. K. Han, J. I. Lee, and J. Jeong, "Study on InGaAsP-InGaAs MQW-LD with symmetric and asymmetric separate confinement heterostructure," IEEE Photon. Technol. Lett. **16**, 1801-1803 (2004).
13. K. H. Schlereth and M. Tacke, "The complex propagation constant of multilayer waveguides: an algorithm for a personal computer," IEEE J. Quantum Electron. **26**, 627-630 (1990).
14. I. K. Han, S. H. Cho, P. J. S. Heim, D. H. Woo, S. H. Kim, J. H. Song, F. G. Johnson, and M. Dagenais, "Dependence of the light-current characteristics of 1.55-μm broad-area lasers on different p-doping profiles," IEEE Photon. Technol. Lett. **12**, 251-253 (2000).